Phys. Chem. Glasses, 2002, **43** (5), ??–???

Glass sintering with concurrent crystallisation. Part 2. Nonisothermal sintering of jagged polydispersed particles

M. O. Prado, C. Fredericci & E. D. Zanotto*[1]

Vitreous Materials Laboratory, Department of Materials Engineering, Federal University of São Carlos - UFSCar, CEP 13.565-905- São Carlos, SP, Brazil

We propose a model, translated into an algorithm, to simulate nonisothermal sintering of polydispersed glass undergoing concurrent crystallisation. The model is based on the two classical sintering stages proposed by Frenkel and Mackenzie–Shuttleworth. The input parameters are green density, particle size distribution, surface tension, viscosity, number of surface nucleation sites (N_s) and crystal growth velocity. We test the model using physical parameters and densification rates for two distinct glasses: a (devitrifying) cordierite glass having a narrow distribution of jagged particles and an alumino-borosilicate glass, ABS (which is stable against crystallisation) having widely polydispersed jagged particles. The experimental densities of the compacts saturate at slightly different values than predicted. Entrapped gases or glass degassing explains the residual porosity in ABS while partial surface crystallisation accounts for density saturation in cordierite glass. The algorithm provides a powerful simulation tool to design the densification of (devitrifying or stable) glass compacts having any particle size distribution, subjected to any heating rate, thus minimising the number of time consuming laboratory experiments.

Relevance, literature review and objectives

The preparation of porous and dense glass articles by sintering is a well established practice in both the laboratory and the industry. However, the development of advanced materials such as sintered glass ceramics, sol-gel derived glasses, amorphous and crystalline thin films and novel metallic alloys, have rekindled the need for a deeper understanding of viscous flow sintering parameters to control spontaneous crystallisation (which hinders sintering) and residual porosity in such materials.[1]

A few models and a variety of experiments have been proposed and conducted on viscous flow sintering. The classical models of Frenkel and Mackenzie–Shuttleworth for the isothermal densification of a porous body, composed of monodispersed glass particles or porous compacts having identical pores, successfully describe parts of the sintering process, e.g. Refs 2–5.

In Part 1,[6] published in this same journal, we reviewed and discussed an algorithm to simulate the kinetics of concurrent isothermal sintering and crystallisation of polydispersed glass particles having no adjustable parameter. The algorithm is based on the two classical sintering models of Frenkel and Mackenzie–Shuttleworth, the JMAK crystallisation theory and in our own model (cluster model) for the sintering of polydispersed particles. The input parameters are particle size distribution (v_r), surface energy (γ), viscosity ($\eta(T)$), number of nucleation sites (N_s) and crystal growth velocity ($U(T)$). We tested the algorithm using experimental data and densification rates on two powdered glasses—polydispersed alumino-borosilicate glass (which is stable against devitrification) and monodispersed cordierite glass (which crystallises easily) at a variety of annealing temperatures, concluding that, despite the simplifications of the cluster model, the agreement between calculated and experimental curves was quite satisfactory. We also emphasised the importance of entrapped gases and degassing on the residual porosity.

In some situations however, depending on the relative rates of heating, sintering, and crystallisation, there may be an onset of these phenomena (or even completion) before the designed annealing temperature is reached. This is particularly true in the case of industrial processes in which large pieces and low heating rates are normally used. Thus it is important to understand and control the sintering and crystallisation process along the heating (and cooling) paths.

To our knowledge very few attempts have been made to describe nonisothermal sintering kinetics of glass powders. In one of the earliest publications on the subject, Cutler[7] described the initial linear shrinkage ($\Delta L/L_0$<15%) of 25×25×4 mm compacts of 15–25 μm diameter soda–lime–silica glass spheres at heating rates of q=0·5–2·9 K/min, up to temperatures varying from 580 to 680°C. Although no corrections were made for particle size distribution and surface crystallisation his experimental data were described by the Frenkel equation. Fortuitously, perhaps, the complications caused by these factors and other experimental errors cancelled out.

Nonisothermal sintering is further complicated by concurrent crystallisation as demonstrated by a few

[1] Author to whom correspondence should be addressed. (e-mail: dedz@power.ufscar.br) * On leave from the Centro Atómico Bariloche -8400 SC de Bariloche- Argentina / Originally presented as an invited paper at the XIX International Congresson Glass, Edinburgh 1–6 July 2001.

authors.[8,9] Boccaccini *et al*,[8] for instance, experimentally demonstrated that cylindrical compacts (5×5 mm) of a crushed Ba–Mg–Al–Si–O glass powder, having a narrow particle size distribution of around 10 μm, could be fully densified when heated at q=15°C/min to 1050°C. However this same powder crystallised and therefore the compact only densified to 89% of the glass density with a heating rate of 1 K/min. Thus a high heating rate privileged sintering over crystallisation.

To the best of our knowledge the only quantitative studies published to date on nonisothermal sintering with concurrent crystallisation are those of Müller *et al*.[9,10] These studies analyse experimental data in the light of existing theories. Müller *et al* used a combination of the Frenkel and MS models (to be discussed later in this article) to describe the sintering kinetics of narrowly distributed, disc milled cordierite glass using an adjustable quantity, defined as the shape parameter, k_s (because the particles were nonspherical). Müller[9] demonstrated that only the compact with the finest particle size tested (r=1 μm) was fully densified at q=12 K/min. Compacts of all the other sizes, from r=3 to 11 μm, crystallised to different degrees and saturated before full densification. Interestingly, they found that k_s~3 for all particle sizes. In conclusion, smaller particles privileged sintering over crystallisation. Corrections for particle size distribution were not made and were thus included in the adjustable parameter k_s. The experimental data[9] will be used throughout this article to test our algorithm.

We presented and tested[6,11] an algorithm that considers sintering with simultaneous crystallisation under isothermal conditions for polydispersed glass powders. As far as we know, however, no one has yet dealt with nonisothermal sintering of polydispersed powders with and without concurrent crystallisation. The objective of this paper is to extend that algorithm and test it for nonisothermal conditions.

We begin by summarising the classical Frenkel (F) and Mackenzie–Shuttleworth (MS) models for sintering spherical, monodispersed, glass particles. We then review our cluster model for the sintering of a compact having a particle size distribution and introduce the problem of concurrent crystallisation (which hinders sintering). Then we derive the densification equations for nonisothermal conditions.

To test the model and the resulting algorithm, we first check them for a nondevitrifying composition, an alumino-borosilicate (ABS) glass having widely polydispersed, jagged particles. We then test both model and algorithm against literature data[9,10] for narrowly distributed cordierite glass powders which have a tendency to crystallise. To conclude we discuss the results of our tests taking into account the assumptions made in the derivations and other complicating factors, such as irregular particle shape, complex crystallisation paths and degassing during sintering.

Summary of the theory

The Frenkel and Mackenzie–Shuttleworth models

The Frenkel model, Equation (1), describes well the isotropic sintering of monodispersed spherical particles.[12] Starting from a compact consisting of loosely packed powder with a relative density of about 0·6, the model works up to a relative density of $\rho=\rho(t)/\rho_g\approx 0{\cdot}8$ (where $\rho(t)$ is the bulk density of the compact and ρ_g the glass density) or, equivalently, up to a linear shrinkage of approximately 10%.

$$\frac{d\left[\frac{\Delta L}{L_0}\right]}{dt}=\frac{3\gamma k_s}{8\eta(T)r} \tag{1a}$$

If shrinkage is isotropic, then

$$\rho=\frac{\rho_0}{\left[1-\frac{\Delta L}{L_0}\right]^3} \tag{1b}$$

where L_0 is the original sample length, ΔL the linear shrinkage after a sintering time t, $\eta(T)$ the temperature dependent shear viscosity, γ the glass vapour surface energy (which is only slightly dependent on temperature), r the initial particle radius, ρ_0 the green density of the compact and k_s is a shape factor (k_s=1 for spherical particles). If the particles are not spherical, k_S is an adjustable parameter.

Using Equation (1a,b) with $C=3k_s\gamma/8r$, the sintering rate for an isothermal process can be rewritten in terms of the relative densities

$$\frac{d\rho}{dt}=3C\rho_0^{-1/3}\rho^{4/3}/\eta(T) \tag{2}$$

For higher relative densities, when spherical pores are isolated in the glass, the Mackenzie–Shuttleworth, MS, model gives the following relationship between densification rate and density[13,3]

$$\frac{d\rho}{dt}=\frac{3\gamma}{2a_0\eta(T)}(1-\rho) \tag{3}$$

where a_0 is the initial radius of the spherical pores. To eliminate the dependence of densification rate on ρ, first one has to integrate Equation (3) and then derive the resulting $\rho(t)$ to obtain another expression for densification rate. In nonisothermal sintering the viscosity should be included as a variable in both derivation and integration steps.

Equation (3) is presented in a simplified form that allows for a simple mathematical treatment.[3] Actually we approximate a to a_0, where a is the pore radius, which is assumed to shrink during sintering, while the number of pores remains fixed. Due to this approximation, Equation (3) slightly underestimates the sintering rate at the end of the process (ρ>98–99%); thus the calculated final density is achieved in a longer time.

These two models describe well the isothermal densification of glass, e.g.[4–7] for the initial F stages and for the final MS stage.[14]

On a laboratory or industrial time scale, sintering is

only accomplished at temperatures above the glass transition, T_g, where the viscosity curve $\eta(T)$ is normally described by the Vogel–Fulcher–Tamman (VFT) equation[15]

$$\eta = \eta_\infty e^{\frac{E_v}{R(T-T_0)}} \quad (4)$$

where R is the gas constant, T_0 is an empirical constant, E_v an apparent activation energy associated to molecular transport by viscous flow, and η_∞ the viscosity at 'infinite' temperature. T_0, E_v, and η_∞ are empirically obtained from shear viscosity measurements. In this paper we use measured values of viscosity as input parameters in the simulations.

The clusters model. Densification of glass with a particle size distribution

Previous studies have demonstrated that the F model describes the initial stage and the MS model describes the final stage of sintering of monodispersed spherical particles.[4–7,14] However, the situation of real powders having a size distribution is more complex. For instance, in a compact of polydispersed particles, after a linear shrinkage of about 8–10%, while the largest particles are at the (initial) Frenkel stage, characterised by the formation of a neck between neighbouring particles, the smaller particles (having a higher specific surface area and thus a higher driving force for sintering) have already passed this stage. This was the basis for the clusters model we had previously proposed:[16] in the initial compact, small particles preferentially cluster in the open spaces left by larger particles and sinter faster. Thus for a polydispersed compact with a volume fraction v_r of spherical particles of radius r, the following expression holds for the densification kinetics at a given temperature.

$$\rho(t) = \frac{\sum_r \left[\begin{array}{l} \rho_F(r,t)\theta_F(t_{0\cdot8}-t)\xi_r \\ +\rho_{MS}(r,t)\theta_{MS}(t-t_{0\cdot8}) \end{array} \right] v_r}{\sum_r \left[\theta_F(t_{0\cdot8}-t)\xi_r + \theta_{MS}(t-t_{0\cdot8})\right] v_r} \quad (5)$$

ξ_r is the neck forming ability of each particle, which can be calculated from the particle size distribution[16] and reflects the effect of mixing particles with different sizes on the sintering kinetics. Equation (5) is slightly different from that used in our previous paper.[16] In this equation, ξ_r only multiplies the Frenkel part of sintering while, in the previous version, ξ_r multiplies both stages of sintering. We believe that this new form is an improvement because ξ_r is calculated from the number of possible contacts between particles (neck forming ability), which exist in the Frenkel stage.

Equation (5) sums up the relative density $\rho(r,t)$ for each particle size, r, as a function of time, t. During the Frenkel stage of sintering, $\rho(r,t)<0{\cdot}8$, and $\rho_F(r,t)$ is calculated using the Frenkel equation, Equations 1(a,b). Later, $\rho(r,t)>0{\cdot}8$, $\rho_{MS}(r,t)$ is calculated by the Mackenzie–Shuttleworth model, Equation (3). For each cluster the transition from the Frenkel regime to the MS regime is made using the step functions $\theta_F(t_{0\cdot8}-t)$ and $\theta_{MS}(t-t_{0\cdot8})$, whose values switch between 1 and 0 at $t=t_{0\cdot8}$ when $\rho_F(r,t_{0\cdot8})=0{\cdot}8$ is reached. Thus, $\theta_F(t_{0\cdot8}-t)=1$ and $\theta_{MS}(t-t_{0\cdot8})=0$ for $t<t_{0\cdot8}$ and $\theta_F(t_{0\cdot8}-t)=0$ and $\theta_{MS}(t-t_{0\cdot8})=1$ for $t>t_{0\cdot8}$. Thus the model for polydispersed spherical particles does not rely on any adjustable parameter. However, for irregular shaped particles, a shape parameter, k_s, must be found empirically for the Frenkel equation (this point will be discussed later in this paper).

The pore radius a_0 in Equation (3) is adjusted to ensure a continuous $\rho(r,t)$ function at $t=t_{0\cdot8}$. The adjustment is achieved by first computing $t_{0\cdot8}$ with Equations (1a,b); then calculating a_0 with the integrated version of Equation (3) at $t=t_{0\cdot8}$. We also checked the effect of forcing the regime transition to occur at $\rho=0{\cdot}75$ instead of at 0·8.

We tested the proposed model with a polydispersed, irregular shaped borosilicate glass powder (which is stable against crystallisation) and determined the densities of uniaxially die pressed cylindrical samples by weighing and measuring their diameters and heights after sequential isothermal heat treatments. The viscosity curve was measured at high temperatures and extrapolated to $T_g \sim 10^{12\cdot5}$ Pa s. The results were well described by Equation (5) using $k_s=1$.[16] However, this value should only hold for spherical particles but the particles used were quite jagged! Due to this surprising result we measured the viscosity at the vicinity of T_g and found a difference from the extrapolated one, Figure 3. Using the new (measured) viscosity data and the modified form of the cluster equation the calculated sintering curves described well the compacts' densification.

Since we derived the cluster model for spherical particles, in this article we compare two different types of calculations for the jagged particles: one with $\xi_r \neq 1$ and $k_s=1$ and other with $\xi_r=1$ and $k_s=1{\cdot}8$ for ABS and $k_S=3$ for cordierite. For ABS the parameter k_s was adjusted using isothermal sintering curves (with $\xi_r=1$) and resulted in a value of 1·8 for the four temperatures tested. For cordierite, k_s was obtained from a fit to the isothermal sintering curves. For sintering in the MS regime k_S is not necessary.

When dealing with monodispersed particles, Equation (5) holds if both ξ_r and v_r are equated to unity and the summation operator is eliminated.

Isothermal sintering with concurrent crystallisation

Most glass powders have a tendency to crystallise from the external surfaces when heated[17] and any fraction of the unsintered surface that crystallises hinders sintering because viscous flow is no longer possible in that part. Thus, it is important to quantify the effect of surface crystallisation on the sintering kinetics. This subject will be summarised in the following section following a more elaborate presentation.[11]

For powdered glasses we assume the most typical case, i.e. instantaneous heterogeneous nucleation of spherical crystals growing on the particle surface with a time independent growth rate $U(T)$ from a fixed number of sites per unit area, N_s. In this case, the JMAK[18] theory predicts the surface fraction crystal-

lised for an infinitely large sample, α_s

$$\alpha_s(t) = 1 - e^{\left(-\pi N_s U(T)^2 t^2\right)} \quad (6)$$

where t is the time of isothermal treatment.

If nucleation is not instantaneous, but continuously progresses with a certain rate up the point when all active sites (N_s) are exhausted, then Equation (6) overestimates the crystallisation kinetics.

Müller *et al*[19] reasonably assumed that (regardless of the sintering model) the densification rate should decrease proportionally to the surface fraction of glass remaining after crystallisation. Thus in this case the isothermal densification rate is

$$\frac{d\rho_c}{dt} = \frac{d\rho}{dt}(1-\alpha_s) \quad (7)$$

where ρ_c is the relative density of a compact which partially devitrifies during sintering.

Inserting the appropriate expressions for $d\rho/dt$, Equations 1(a,b), (3) and α_s, Equation (6), into Equation (7), and upon integration, one arrives at Equations (8) and (9) for the Frenkel and Mackenzie–Shuttleworth cases, respectively

$$\rho_{c,F}(t) = \frac{\rho_0}{\left[1 - \frac{C}{\eta(T)}\int_0^t e^{-\pi N_s U(T)^2 t^2}\, dt'\right]} \quad (8)$$

$$\rho_{cMS}(t) = \rho_0 + (1-\rho_0)\left(\frac{C'}{\eta(T)}\right)\int_0^t e^{\left\{\frac{-C't'}{\eta(T)}\right\}} e^{-\pi N_s U(T)^2 t'^2}\, dt' \quad (9)$$

where $C' = (3\gamma/2a_0)$.

Nonisothermal densification kinetics

In some situations, however, depending on how fast the sintering and crystallisation rates are, a substantial part of these processes may occur on the heating path before the specimens reach the desired treatment temperature. Thus it is fundamental to simulate which sintering and crystallisation degrees are achieved at a given heating rate just before the designed annealing temperature is reached.

The time, t, may be treated as a temperature dependent variable, $dt = dT/q$, where q is a constant heating rate. Making the appropriate changes of variables, the temperature dependent crystallisation, i.e. the surface fraction crystallised as a function of heating rate, can be written as follows:

$$\alpha_s(T) = 1 - e^{-\pi \frac{N_s}{q^2}\left(\int_{T_g}^{T} U(T')dT'\right)^2} \quad (10)$$

where T_g is the glass transition temperature and T is the final temperature reached at the end of a continuous heating sintering experiment.

The densification rates for both F and MS stages may be similarly written.

From Equations (1a), (7), (10) one arrives at Equations (11) and (12), respectively

$$\frac{\Delta L}{L_0}(T) = \frac{C}{q}\int_{T_g}^{T} \frac{1-\alpha_s(T')}{\eta(T')} dT' \quad (11a)$$

which, together with Equation (1b), gives the Frenkel sintering kinetics concurrent with surface crystallisation for an isotropic nonisothermal process, (11b)

$$\rho(T) = \frac{\rho_0}{\left[1 - \frac{C}{q}\int_{T_g}^{T} \frac{1-\alpha_s(T')}{\eta(T')} dT'\right]^3} \quad (11b)$$

The corresponding MS expression, obtained from Equations (3), (7), (10), is

$$\rho_{c,MS}(T) = \rho_0 + (1-\rho_0)\left(\frac{C'}{q}\right)\int_{T_g}^{T} \frac{e^{\left(\frac{-C'}{q}\int_{T_g}^{T}\frac{dT}{\eta(T)}\right)}\left(1-\alpha_s(T')\right)}{\eta(T')} dT' \quad (12)$$

With these equations and the appropriate physical parameters of the glass (particle size distribution, green density, surface tension, viscosity vs temperature, number of active nucleation sites per unit surface and crystal growth rate vs temperature) it is possible to predict the densification kinetics; ρ or ρ_c vs time or temperature. Except for $U(T)$, which must be measured, the other parameters can be estimated from the glass composition (η, γ) or they can be used as simulation parameters (N_s, v_r, ρ_0).

Polydispersed distributions undergoing sintering and concurrent crystallisation can be treated by introducing Equations (11) and (12) into Equation (5).

Materials and methods

We used two distinct glasses to test the proposed model. The first one was an alumino-borosilicate glass (ABS), which is stable against crystallisation, having widely polydispersed jagged particles. The second one consisted of narrowly distributed size fractions of (devitrifying) cordierite glass powder, with average radius from 1 to 11 μm. Table 1 shows their chemical compositions.

To use the model we employed literature data for cordierite[9] and determined several parameters for the ABS glass: particle size distribution, green density (ρ_o), glass density (ρ_g), body density ($\rho(T)$), viscosity ($\eta(T)$), crystal growth rate ($U(T)$) and total number of nu-

Table 1. *Chemical compositions of ABS and cordierite glasses (wt%)*

Glass	SiO_2	B_2O_3	Na_2O	CaO	Al_2O_3	MgO
Cordierite	51·4	–	–	–	34·9	13·8
ABS	71·7	8·3	7·4	2·7	8·6	1·0

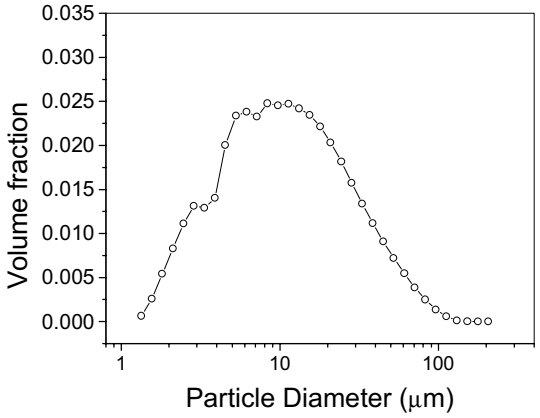

Figure 1. *Size distribution of the ABS glass particles. The curve was normalised in such a way that the area under it is unity*

cleation sites per unit area (N_s).

Particle size distribution, v_r

We measured the particle sizes for the ABS glass with a Mastersizer μ Ver 2.0. Figure 1 shows the obtained size distribution.

For the cordierite glass, almost monodispersed particles having 1, 6·8, 8 and 11 microns[9] were considered in the simulations.

Glass compacts

In the case of ABS glass, cylindrical powder compacts were uniaxially die-pressed at 0·5 MPa for 30 s without binder. Around 0·75 g of glass powder were used for each sample. The cylinders were approximately 6 mm high and 10·2 mm in diameter. The sample's length and diameter were measured with a micrometer to determine its green density.

The data taken from Reference 9 for cordierite glass correspond to isostatically pressed samples at 200 MPa, using no binder, which resulted in cylindrical compacts of diameter d=8 mm and height l=5 mm.

Glass density, ρ_g

We measured ABS's true density (ρ_g=2·360 g/cm^3) by He pyknometry, using an AccuPyc 1330 Micromeritics pyknometer, and used this value for the calculation of the relative density. The relative densities of cordierite glass after nonisothermal treatments at 12 K/min were taken from Reference 9.

Glass transition temperature, T_g

We determined the glass transition temperature of ABS by differential scanning calorimetry using a Netzsch DSC, Model 404 calorimeter. The glass particles used were <74 μm and the heating rate was 10 K/min, T_g~848 K. For stoichiometric cordierite T_g~1082 K.

Viscosity, $\eta(T)$

We performed low temperature viscosity measurements (up to 1090 K) by the penetration method. High temperature viscosity was determined by the rotating cylinder method in a Theta viscometer, with a maximum temperature of 1600°C. We obtained the viscosity curve by fitting the Vogel–Fulcher–Tamman equation ($\log\eta = A + B/(T - T_o)$) to both low and high viscosity data. We found A=–2·086, B=4983·2 and T_o=510·5 K for the ABS glass. Figure 2 shows the measured viscosity and fitted curve for the ABS and cordierite.[9] The equation reported for cordierite glass is $\log\eta = -1{\cdot}96 + 4265/(T - 777)$ (η[Pa s], T [K]).[9]

Crystal growth rate , U(T)

Müller[9] reported that the crystal growth rate of μ-cordierite in cordierite glass is $U(T) = 5\times10^9\, e^{(-415{,}000/R.T)}$ m/s with R=8·314 J/mol K. This equation is valid in a relatively narrow temperature range where sintering occurs in laboratory time scales.

Sintering of the compacts, $\rho(T)$

The ABS compacts were sintered in air, at final temperatures of about 1100 K (T_g~848 K). The measured heating rates were q=1·1 and 5·3 K/min for ABS and 12 K/min for cordierite. After reaching the desired temperatures (previously designed with our algorithm) the samples were air quenched to room temperature to preclude any additional sintering on the cooling path. The sintered compact densities were determined by the Archimedes method using mercury displacement on a precision scale. For cordierite, Müller[9] measured the axial shrinkage in a hot stage microscope and transformed these data into density by using Equation (1b). The final (saturation) values were checked by independent density measurements.

Number of crystals per unit area (N_s*)*

For cordierite glass N_s was estimated from the following expression

$$N_s \approx \frac{1}{(2r)^2} \tag{13}$$

where r is the average radius of the crystals at the moment they impinge on each other.

The value of r was estimated from Equation (14).

$$r(T_i) = \frac{1}{q}\int_{T_g}^{T_i} U(T)\,dT \tag{14}$$

where $U(T)$ is the crystal growth rate and T_i the temperature of impingement. This impingement temperature was estimated as follows. From the nonisothermal sintering data[9] for a given particle size we obtained the temperature corresponding to the point where the compact density reached its maximum value (where crystallisation clearly arrested sintering before full densification). With this temperature we estimated a lower bound for N_S. In addition, an upper bound for N_S was calculated at the temperature were the Frenkel regime begun to slow down due to crystallisation. The calculated average is $N_S = 1{\cdot}09\times10^{11}$ m^{-2}.

The values of the glass vapour surface energies were γ_{ABS}=0·327 and γ_{Cor}=0·360 J/m^2, both assumed temperature independent.

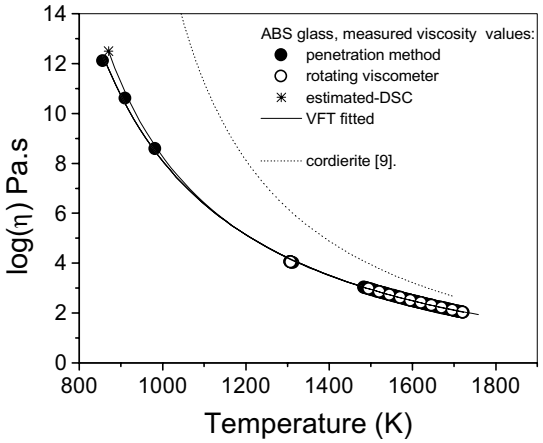

Figure 2. *Viscosity of ABS (measured) and cordierite (calculated) glasses*

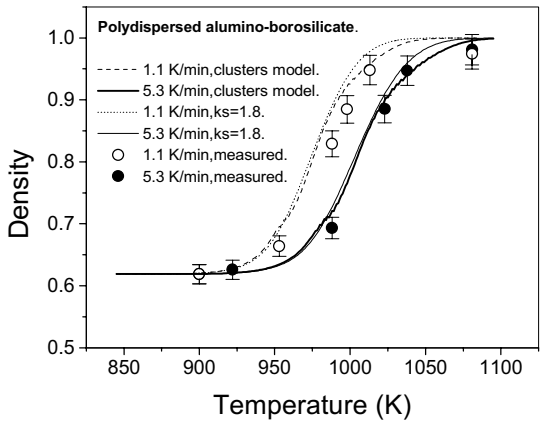

Figure 3. *Calculated (lines) and experimental (circles) densification curves of ABS glass for two heating rates:* q_1*=1·1 K/min (dot line and hollow circles) and* q_2*=5·3 K/min (full line and solid circles)*

Simulations and test of the model with two glasses

We tested with two distinct glasses an algorithm based on Equations (5), (11), (12) which was constructed using commercial software.

Alumino-borosilicate glass with a wide size distribution of jagged particles

We first used the ABS glass with a wide size distribution of jagged particles (Figure 1). We chose this system to limit the number of variables to a controlled level because it is stable against crystallisation. Thus in principle viscous sintering would proceed undisturbed until full densification was reached.

Figure 3 shows the calculated and experimental densification curves for two heating rates. Due to the uncertainty caused by the unknown shape factor of the jagged particles, we present two types of calculated curves. One results from the cluster model, Equations (5), (11), (12), with k_s=1 and $\xi_r \neq 1$ (calculated from the particle size distribution without any adjustable parameter[16]) while the other curve results from k_s=1·8 (fit to isothermal data[16] for the same glass powder) and ξ_r=1. For both heating rates there is a small temperature shift between experimental and calculated curves of about 5–10 K. The experimental density saturates at about ρ~98%. Negligible level of crystallisation was observed at the temperature of maximum density for each heating rate. Some possible explanations for the saturation density will be discussed later.

Cordierite glass/narrow distribution of crystallising particles

To further test the algorithm under more strict conditions, we also worked with a cordierite glass having a relatively narrow distribution of jagged particles. This glass has a tendency to devitrify concurrently with sintering; thus we hoped to examine our model under this arresting condition.

Figure 4 shows the calculated (this work) and experimental[9] densification curves of cordierite glass having average particle sizes r=1, 6·8, 8 and 11 μm, subjected to a heating rate of 12 K/min. The crystallised surface fraction is also shown. In these conditions crystallisation starts at ~1150 K and is completed at ~1250 K. At this point densification is completely arrested.

Due to the unknown shape factor of the jagged particles, we used it as a fitting parameter, resulting in k_s~3. Only the finest particles fully densify, all the other curves saturate at ρ~0·84, 0·82 and 0·80 (calculated curves) or at ~0·85, 0·80 and 0·75 (experimental data) for increasing particle size, demonstrating the arresting effect of crystallisation.

In all cases the experimental density saturates at slightly different values than predicted. If one forces the passage from the Frenkel to the MS regime to occur at 0·75 instead of at 0·8 a better agreement is found for the two largest particle sizes but not for the smallest. Some possible explanations for these differences will be discussed later.

Discussion

We will now discuss the main results in light of the assumptions made throughout the article.

The proposed model and the resulting algorithm were tested under strict conditions. Figure 3 (ABS) and Figure 4 (cordierite) show a pattern consisting of two similar features for both glasses, despite their significant compositional and geometrical difference (a crystallising glass having a narrow distribution of jagged particles and a stable glass having a large distribution of jagged particles). First, the experimental and calculated curves coincide or are parallel indicating that, before saturation, the temperature dependence of nonisothermal sintering kinetics is well predicted by our algorithm. Second, the compacts' measured saturation densities differ somewhat from the predicted values.

The fact that our simulations slightly overestimate the nonisothermal sintering kinetics (but predict well the isothermal sintering kinetics of the noncrystallising ABS[6,16] may be attributed to a number of causes: assumptions of the model, underestimated crystallisation degree due to errors in the input parameters (number of surface nucleation sites and crystal growth velocity) or in the validity of the JMAK equation, errors in other input parameters (particle size distribution, surface tension or viscosity), entrapped gases or

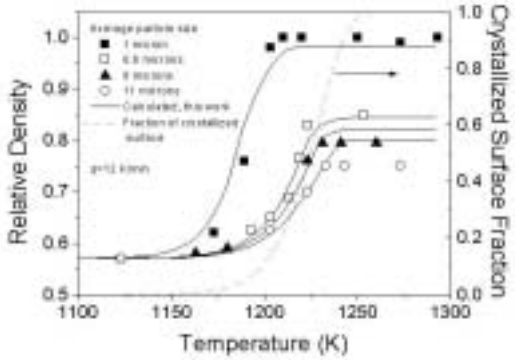

Figure 4. *Simulated (solid lines, this work) and experimental (from Reference 9) densification curves for nonisothermal sintering of cordierite glass powders of different sizes. The crystallised surface fraction (dotted line) is also shown*

degassing. These possible causes will be described and tested in the following paragraphs.

Particle geometry, the shape factor

The Frenkel equation was derived for monodispersed spherical particles in the initial stages of sintering. However in most practical situations, such as those reported in this article, ground (jagged) particles are used. Cutler[20] long ago demonstrated that, in the Frenkel stage, jagged particles of soda-lime-silica glass sinter about 5 times faster than do spheroidised particles of the same glass. Thus, a k_s=5 would be necessary to bring his experiments and theory into agreement. Obviously this effect depends on how the actual particle shape departs from spheroidicity.

It is reasonable to expect that the particle shape may have a significant effect on sintering only during the Frenkel stage since, at these early stages, necks begin to form and the original shape (radius of curvature) of the particles is still conserved. Every ground particle has surfaces with a variable radius of curvature. Hence, the initial kinetics of sintering is determined by the distribution of different contacts formed among them. Assuming that there is no memory of the original factor k_s has to be used in the Frenkel equation.

Due to the uncertainty caused by the unknown shape factor of the jagged particles, we present two types of calculated curves for ABS. One results from the cluster equation, Equations (5), (11), (12), with k_s=1 and $\xi_r \neq 1$ (calculated from the particle size distribution without any adjustable parameter[16]) while the other results from the cluster equation with k_s=1·8 (fit to isothermal data for the same glass powder) and ξ_r=1. There is a slight difference between the two calculated curves (Figure 3). However, only the first has a predictive power, because it uses no adjustable parameter. To decide how accurate is our approach (ξ_r), we plan to carry out an isothermal study of spherical, noncrystallising glass in the near future.

As the shape factor of cordierite was unknown, we used it as a fitting parameter to the nonisothermal densification data resulting in k_s~3, in agreement with the published value[9]. Since k_s was fitted to bring the experimental and calculated curves into agreement in the Frenkel regime, errors in this parameter cannot explain the differences in the final (saturation) densities.

The fact that k_s=5 for Cutler's glass[20] k_s=3 for cordierite, k_s=1·8 for ABS and k_s=1 for spherical particles indicates that this parameter strongly depends on the particle geometry. Therefore, irregular particles apparently present higher sintering rates than spherical particles.

Errors in the calculated crystallisation kinetics

Is nucleation instantaneous from a fixed N_s*?* We assumed the most typical case, i.e. instantaneous heterogeneous nucleation of spherical crystals growing on the particle surface with a growth rate $U(T)$ from a fixed number of sites per unit area, N_s. However:

1. if nucleation is not instantaneous, but continuously progresses with a certain rate up the point when all active sites (N_s) are exhausted, then Equation (6) overestimates the crystallisation kinetics;
2. in addition, a second effect may change the total number of active sites. In the typical case, when most active surface nucleation sites are solid impurities, N_s is constant throughout sintering and these solid particles will remain active even after the original grain surfaces have disappeared. These engulfed impurities continuously contribute to the crystallisation of the 'ghost' surfaces but do not impair sintering. The remnant impurities on unsintered parts of the original surfaces continuously arrest sintering but this is taken care of by the model. On the other hand, when a substantial fraction of N_s is composed of scratches and edges[17] these active sites (engulfed or not) will tend to round off and disappear during sintering, no longer contributing to crystallisation. Therefore, in the case of scratches and edges, if N_s is kept constant in the calculations, the crystallisation kinetics will be overestimated. Therefore, effects (1) and (2) overestimate crystallisation and hence the sintering kinetics will be underestimated.

Apparently this is not the case here because the calculated final densities are slightly smaller than the experimental values for particles of 1·0 and 6·8 μm and larger for the other particle sizes.

Nonvalidity of the JMAK equation for small particle size. In the case of small glass particles, such that the combination of N_S and particle size results in one or less nucleation sites per particle, departures are expected from the JMAK behaviour. This is the case, for instance, for particles with a radius of $\approx 10^{-6}$ m and $N_S \approx 10^{11}$ m^{-2} used by Muller.[9] In this typical case each crystal grows without interacting with other crystals and thus crystallisation is only limited by the borders of the particle on which it is growing.

Figure 5 shows the numerically computed surface crystallisation kinetics and that obtained by the (inadequate) use of the JMAK Equation (6) for disc milled cordierite particles having ρ=1 μm, treated at 1273 K, where the growth rate of crystals is approximately 0·05 micron/s and $N_S \approx 10^{11}$ m^{-2}. Similar results are obtained with both approaches for low α_S but for α_S>0·3 the

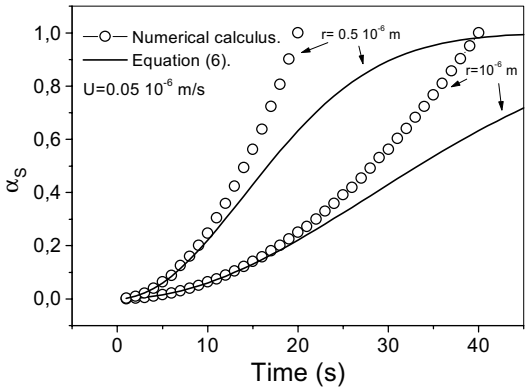

Figure 5. *Crystallised surface fraction of 1·0 and 0·5 micron size spherical particles,* $N_S=1/(4\pi r^2)$ *and* $U=0{\cdot}05\times10^{-6}$ *m/s. Numerical calculation (circles) and values obtained with Equation (6) (lines)*

actual kinetics are faster than that obtained with Equation (6) and thus the crystallisation of fine powders may be faster than that of average or larger particles.

For the cordierite glass powders used in this study with $r>1$ μm several sites existed per particle and therefore this correction was unnecessary. However, Equation (6) underestimates the crystallisation kinetics for the smallest particles, $r=1$ μm.

The crystal morphology. Another source of error in estimating the crystallised surface fraction is that μ-cordierite crystals are not spherical.

Therefore, there are several problems concerning the direct use of Equation (6) to estimate the crystallised fraction and these factors may cause errors in the calculated sintering kinetics.

Residual porosity

Residual porosity is a recurrent problem regarding viscous flow sintering. The results of several authors, as well as our own, show that it is very difficult to achieve full densification even in the absence of crystallisation.

Compacts of ABS glass saturate at $\rho\sim0{\cdot}96$–$0{\cdot}98$ for both isothermal[6,16] and nonisothermal heating (this work) but in general our simulations predict slightly higher final densities. It should be pointed out again that MS Equation (3) slightly underestimates the sintering rate at the very end of the process; thus maximum density is (theoretically) achieved in a larger time than it should. But, in the absence of crystallisation, the exact expression also predicts full densification. Therefore this approximation is not responsible for the missfit to the experimental density.

At least three factors can cause residual porosity: partial or total surface crystallisation, bubble formation due to the release of dissolved gas (which can be catalysed by crystallisation) and entrapped insoluble gases in the initial pores. For instance water vapour and air (particularly N_2) have low solubility in silicate glasses. While the first cause—partial surface crystallisation—is taken into account in our equations, the other two are not.

Alumino-borosilicate glass. ABS glass does not easily crystallise at the heating rates and final temperatures used. Thus, saturation of the sintering curves at ~96–98% cannot be assigned to crystallisation.

Gaber *et al*[21] stated that water, nitrogen and carbon oxides (CO, CO_2) outgo the sintering particles of soda–lime–silica glass with a dynamics that depends upon the particle size. Adsorbed gases on particle surfaces are eliminated at low temperatures but gases dissolved in the interior of glass are released with more difficulty by bigger particles (this is a diffusion process). At a constant heating rate, larger particles release this type of gas at higher temperatures. Additionally crystallisation may induce gas release due to the different solubility of gases in the crystalline and vitreous phases. These gases may increase the porosity of the compact if they emerge during sintering.

With the barely crystallising ABS glass, about 2–4% of closed pores always remained in the glass regardless of the sintering temperature (isothermal treatments) or heating rate (nonisothermal). Therefore, the remaining pores are related to entrapped gases or glass degassing.

Cordierite glass. The data[9] for $r=1$ μm indicate high densification. Thus no degassing or entrapped gases existed in this glass. This is a quite rare event. We were not able to fully densify three types of glasses, including ABS and two families of soda–lime–silica glasses.

Therefore, the saturation at $\rho<1$ observed for larger particle sizes is clearly due to surface crystallisation. Hence in order to fully densify cordierite glass, the particle size must be reduced. In practical situations, however, fine particles may hinder powder flow into moulds in industrial operations. An alternative way is to submit coarse fragments of glass to high energy milling for very short times to reduce N_s.[9]

Despite the theoretical and experimental problems discussed in this article, we have demonstrated the general ability of the model and algorithm to predict (within acceptable limits) nonisothermal sintering with or without concurrent crystallisation. The model allows one to calculate the appropriate thermal path (heating rate and final temperature) in order to obtain the desired porosity and crystallinity of the compact. Based on the values of v_r, $\eta(T)$, γ, ρ_g, N_s and $U(T)$ as inputs, $\rho(T,q)$ and $\alpha_s(T,q)$ or $\alpha_v(T,q)$ curves can be calculated for different heating rates.

Conclusions

We have developed a model to predict the nonisothermal sintering kinetics of polydispersed glass compacts with or without concurrent crystallisation. The model was tested under strict conditions with two systems: a crystallising glass having a narrow particle size distribution and a stable glass having a large size distribution.

Despite the substantial compositional and geometrical differences of the two glasses, before saturation, the experimental and calculated densification curves coincide (for cordierite) or are parallel (for ABS) within the error limits, indicating that the temperature dependence of nonisothermal sintering kinetics is predicted by the model.

The other interesting result of this research is that, even for the noncrystallising ABS glass, the compacts' density saturates at slightly lower density than predicted by the simulations. This saturation may be due to at least three factors: partial or total surface crystallisation, entrapped insoluble gases in the initial pores and bubble formation owing to dissolved gas release (which can be catalysed by crystallisation). While the first cause—surface crystallisation—is taken into account by the model equations, the remaining two are not. Partial crystallisation explains the residual porosity in cordierite while entrapped gases or degassing cause the remnant porosity in ABS glass.

The algorithm provides a powerful simulation tool to design the densification of glass compacts having any particle size distribution subjected to any heating rate thus minimising the number of time consuming laboratory experiments.

Acknowledgements

To CONICET and Comisión Nacional de Energía Atómica (Argentina) and CNPq, Cyted, Pronex, Fapesp (Brazil) for funding this research.

References

1. Rabinovich, E. M. Preparation of glass by sintering. *J. Mater. Sci.*, 1985, **20**, 4259.
2. Giess, E. A., Fletcher, J. P. & Wynn Herron, L. Isothermal sintering of cordierite-type glass powders. *J. Am. Ceram. Soc.*, 1984, **67** (8), 549.
3. Yet-Ming Chiang, Birnie, D. P., III & Kingery, W. D. Single phase sintering. In *Physical ceramics. Principles for ceramic science and engineering*. 1997. John Wiley & Sons Inc, New York. Pp 392–8.
4. Kuczynski, G. C. Study of the sintering of glass. *J. Appl. Phys.*, 1949, **20** (12), 1160–3.
5. Kuczynski, G. C. & Zaplatynskyj, I. Sintering of glass. *J. Am. Ceram. Soc.*, 1956, **39** (10), 349–50.
6. Zanotto, E. D. & Prado, M. O. Isothermal sintering with concurrent crystallization of monodispersed and polydispersed glass particles. Part 1. *Phys. Chem. Glasses*, 2001, **42** (3).
7. Cutler, I. B. Sintering of glass powders during constant rates of heating. *J. Am. Ceram. Soc.*, 1969, **52** (1), 14.
8. Boccaccini, A. R., Stumpfe, W., Rtaplin, D. M. & Ponton., C. M. Densification and crystallization of glass powder compacts during constant heating rate sintering. *Mater. Sci. Eng. A*, 1996, **219**, 26–31.
9. Müller, R. On the kinetics of sintering and crystallization of glass powders. *Glastech. Ber. Glass Sci. Technol.*, 1994, **67C**, 93–8.
10. Müller, R., Reinsch, S. & Gaber, M. Sinterability of glass powders. *Glastech. Ber. Glass Science Technol.*, 2000, **73C1**, 205–12.
11. Prado, M. O., Fredericci, C. & Zanotto, E. D. Isothermal sintering with concurrent crystallization of soda-lime-silica glass beads. *J. Non-Cryst. Solids*, Submitted 2002.
12. Frenkel, J. Viscous flow of crystalline bodies under the action of surface tension. *J. Phys. USSR*, 1945, **9** (5), 385.
13. Mackenzie, J. K. & Shuttleworth, R. A phenomenological theory of sintering. *Proc. Phys. Soc. Lond. B*, 1949, **62**, 833.
14. Scherer, G. W. Sintering of gels. In *Sol-gel science and technology*. 1989. Edited by M. A. Aegerter & E. D. Zanotto. World Scientific Publishing Co. Ltd., New Jersey. Pp 221–56.
15. Gutzow, I. & Schmelzer, J. The viscosity of glass-forming melts. In *The vitreous state. Thermodynamics, structure, rheology and crystallization*. 1995. Edited by Springer, Berlin. Pp 32–40.
16. Prado, M. O., Zanotto, E. D. & Müller, R. Model for sintering polydispersed glass particles. *J. Non-Cryst. Solids*, 2001, **279** (2–3), 169.
17. Müller, R., Zanotto, E. D. & Fokin, V. M. Surface crystallization of silicate glasses: nucleation sites and kinetics. J. *Non-Cryst. Solids*, 2000, **274** (1–3), 208–31.
18. Weinberg, M. C. Surface nucleated transformation kinetics in 2- and 3-dimensional finite systems. *J. Non-Cryst. Solids*, 1991, **134**, 116–22.
19. Müller, R., Kirsch, M. & Lorenz, H. Surface crystallization, a limiting effect of sintering glass powders. *15th Int. Congr. on Glass*. Leningrad. Vol. 3. 1989. P 334.
20. Cutler, I. B. Effect of particle shape on kinetics of sintering of glass. *J. Am. Ceram. Soc.*, 1968, **51** (10), 604.
21. Gaber, M., Müller, R. & Hölland, W. Degassing phenomena during sintering and crystallization of glass powders. *Proc. Sixth Int. Otto Schott Colloquium*, Jena. 1998. *Glastech. Ber. Glass Sci. Technol.*, 1998, **71**C, 353.